J Electr Eng Technol.2018; 13(3): 1346-1354
http://doi.org/10.5370/JEET.2018.13.3.1346

ISSN(Print) 1975-0102
ISSN(Online) 2093-7423

# Cost Effective Design of High Voltage Impulse Generator and Modeling in Matlab

**Zahid Javid*, Ke-Jun Li†, Kaiqi Sun* and Arooj Unbreen****

**Abstract** – Quality of the power system depends upon the reliability of its components such as transformer, transmission lines, insulators, circuit breakers and isolators. The transient voltage due to internal or external reasons may affect the insulation level of the components. The insulation level of these components must be tested against these conditions. Different studies, testing of different electrical components against high voltage impulses and different industrial applications rely on the international manufactures for pulsed power generation and testing, that is quite expensive and large in size. In this paper a model of impulse voltage generator with capacitive load of pin type insulator is studied by simulation method and by an experimental setup. A ten stage high voltage impulse generator (HVIG) is designed and implemented for different applications. In this proposed model, the cost has been reduced by using small and cheap capacitors as an alternative for large and expensive ones while achieving the same effectiveness. Effect of the distributed capacitance in each stage is analyzed to prove the effectiveness of the model. Different values of front and tail resistances have been used to get IEC standard waveforms. Results reveal the effectiveness at reduced cost of the proposed model.

**Keywords**: Capacitive energy storage, Dielectric breakdown, Impulse testing, Insulation testing, Voltage multiplier.

## 1. Introduction

High voltage impulse generator has many applications in industrial, biological, environmental and defense related fields, such as pollution control, electrostatic precipitation, high power microwave, flashed X-ray in industry, eye surgery and bone repair in medicine. This paper focuses on the applications of high voltage impulse generator in the field of electrical power industry. Both overhead transmission and distribution lines are exposed to different environmental conditions during their life span, including lightning strokes, which represent one of the severe stresses on electrical equipment[1].

The second cause of impulse generation in power system is load switching. The core distinctiveness of lightning strikes is over voltages with high amplitudes and rapid rates of rising, as shown in Fig. 1. It is classified as rapid front over voltages with front times varying from 0.1 to 20 μs & tail time of 50 μs(1.2/50 μs standard lightning waveform) [2]. While for the switching impulse it is 250/2500 μs [2, 3]. The insulation level of the power system components should be tested against these conditions. Lightening protection devices are developed to redirect the lightning strokes, to shield the system from insulation failure. These protection devices must be tested to make sure their reliable operation against these conditions. To test these devices, artificial testing equipment is needed which can generate the same conditions in the laboratory. Many researchers discussed different approaches [4-7] to generate these artificial conditions for testing purpose.

There are different types of high voltage impulse generators that can generate high-voltage pulses, such as Tesla-type SOS-type (semiconductor opening switch), LTD

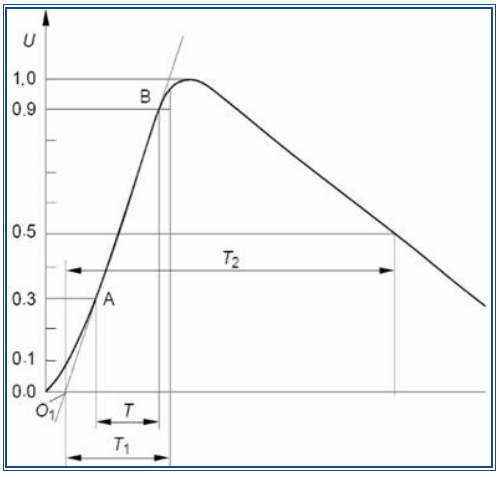


**Fig. 1.** IEC standard lightening impulse wave form [front time: $T_1$=1.67 x T=1.2 μs ±30 %, tail time: $T_2$=50 μs ± 20 %]

† Corresponding Author: School of Electrical Engineering, Shandong University, China. (lkjun@sdu.edu.cn)
* School of Electrical Engineering, Shandong University, China. (zaifuu4444@gmail.com, skqlxf@qq.com)
** Dept. of Electrical Engineering NFC IE&FR Faisalabad, Pakistan, (aroojunbreennfc@gmail.com)
Received: August 2, 2017; Accepted: January 10, 2018

(linear transformer driver) & Marx generator [8]. Tesla-type impulse generator cannot generate impulses with the rapid rate of rising and falling edges. SOS-type impulse generator can generate impulses with rapid rate but their efficiency is very low. LTD generators have low efficiency and big sizes.

In comparison with these generators, Marx generators is the best choice because it can generate very high voltage (>100 KV) impulses at high efficiency and with a rapid rate [9]. Nowadays generalized Marx topology is proposed and proved to be feasible [10]. Measurement of the dielectric properties of nonlinear grading elements is best carried out using an impulse generator The simplicity of the circuit configuration and feat of the Marx impulse generator, enable its usage in a wide range of application such as science, military, insulation testing etc. Its topology is simple which includes capacitors, resistors and sphere gaps as switches.

Haitao Li [11] developed a pulsed power supply consisting of several superconducting pulsed power transformers with Marx generator methodology. His experimental and simulation results shows that proposed design can meet the requirements of basic experimental study for a small rail gun but not enough for real testing. Yuan Xuelin [12] proposed a solid state pulser based on avalanche transistor Marx circuit. In which avalanche transistor is used as a switch, it can generate high-repetition and stable short-pulses, but its power is not enough for testing purpose, in order to increase the power of the circuit he introduced charged capacitors in the Marx circuit which is very inconvenient in terms of practical circuit.

The Marx impulse generator was introduced in 1923[2, 13]. It`s working principle is to charge the capacitors in parallel and discharge them in series that produces an high voltage impulse of short duration by adding up the voltages of all the capacitors [2, 14]. The rising and falling time of the output impulse can be controlled by using different values of front and tail resistors. Various attempts were made to improve the performance and extend the topology of the Marx circuit but the main problem was the cost and size of the generator [15, 16].

The current efforts are focused to transform it into portable and small in size and also cost effective. However, the main mechanism of this circuit remains the same. Contingent upon the purpose it is essential to understand more about the Marx basic circuit, relationship between energy stored, input voltage, capacitor values, the number of stages and their effects on the cost. Although, hypo-thetically any output voltage and energy for a Marx impulse generator can be expected.

The standard values of capacitors, breakdown voltages, size and their cost limits the viability of the desired output and design. Based on above-cited factors this paper focused on the design of impulse voltage generator which is cost efficient and compact in size.

Arash Toudeshki [17] has presented the algorithm for

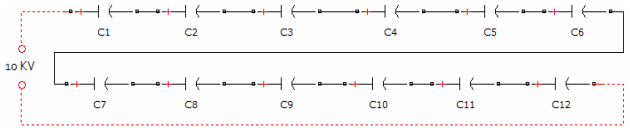


**Fig. 2.** Capacitor bank arrangement

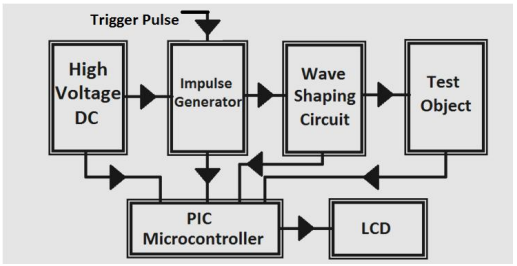


**Fig. 3.** Block diagram of the system

cost calculation and the factors that affect the cost of the Marx impulse generator. Joe Y. Zhou[18] discussed in his paper about very low energy laboratory impulse generators which can be used to test laboratory scale samples.

In under discussion system insulation problems of the structure, controllability, observability, stability and efficiency of the system are also discussed in addition to its cost and size. High voltage capacitors are the most expensive components of the Marx impulse voltage generator.

Fig. 2 shows that how capacitor arrangements were used to make the system cheaper. Instead of using one high voltage capacitor small capacitors were coupled in a string to get the same effect with lower cost.

Fig. 3 represents block diagram of the system. The system is divided into five main parts; 1-High Voltage Direct Current (HVDC) supply 2-Impuse Voltage Generator (IVG) 3-Wave shaping circuit 4-Test object (11KV pin type insulator) 5- Display.

Rest of the paper is organized as follows. The detailed design of the system is described in section II, while section III is about the analysis of the system. Section IV reflects the experimental and simulation results finally section V is comprises of conclusions based on the simulation and practical results.

## 2. Design

### 2.1 High voltage DC supply

Various techniques were studied in the first phase to generate HVDC up to 10KV. Prototype hardware was developed using Cockcroft-Walton voltage multiplier (CWVM) technic. This technique was used because the designed set was intended to be applied for the charging of IVG. The key components for the erection of high Voltage DC power supply are; transformer, power diodes, inverter

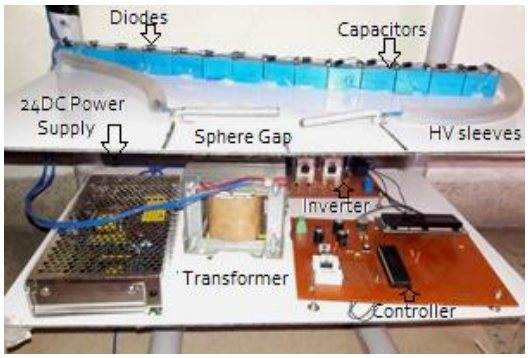


**Fig. 4.** High Voltage DC supply (CWVM technique)

and capacitors. Eq. (1) shows the inverse relation between frequency and voltage drop so high-frequency transformer (9 kHz) was used to decrease the losses [2] Here ΔV: voltage drops, f: supply frequency, C: capacitance and n: no of stages.

$$\Delta V = \frac{\mathrm{I}}{fC}\left(\frac{2}{3}n^3 - \frac{n}{6}\right) \quad (1)$$

Joseph, M.B [19] has presented the fundamental process of multiplier circuit and discussed the guidelines for the selection of capacitors and diodes. Spencer[20] have designed a prototype of surface mounted Cockcroft-Walton board. The advantage of this set is low cost, high reliability, portability and simple control. The proposed model of HVDC is shown in Fig. 4. This model consist of; 28 no of stages (each capacitor is 0.68uF, 600V), diode (DGP-30 with 6 ampere current rating). The output of the model is 9.98 KV.

## 2.2 Impulse voltage generator

The next step of this work was to design the impulse generator. It was very critical part of the work not only with respect to its cost but also due to its design and operation. Various attempts were made to reduce the cost; one is to use small rating capacitors instead of one big size high voltage capacitor for each stage. Fig. 5. depicts the proposed model, made up of 12 capacitors to make a single stage of the impulse generator. Each capacitor is rated at 1KV, 220nF, so each stage is rated at 18.33nF, 12 KV. The reason of connecting 2 extra capacitors in each string is to evade over stressing of any capacitor in the string. As the desired output was 95 KV (required for the testing of 11KV electrical equipment), so 10 stages were connected with 10KV DC charging voltage.

The critical design parameters of the generator are its structure, sphere gaps, capacitor banks and wave shaping circuit [21, 22]. The whole structure was made of Bakelite and polyvinyl chloride (PVC) material. Adjustable sphere gaps were made using copper rods and copper semi-circles as shown in Fig. 6. This type of assembly is very helpful

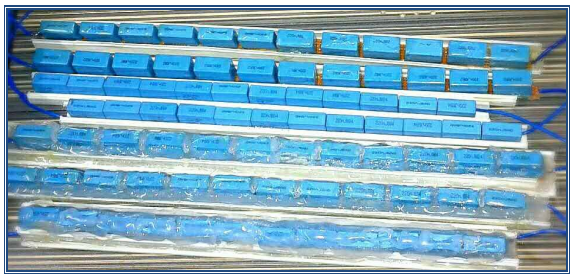

**Fig. 5.** Arrangement of a 10 kV high voltage capacitor

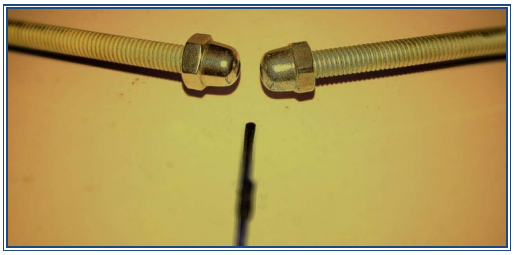

**Fig. 6.** Sphere gap

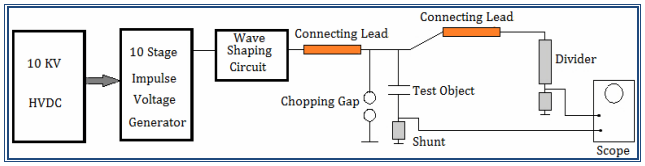


**Fig. 7.** Schematic diagram

to regulate the breakdown voltage of the gaps, as the breakdown voltage between sphere gaps change rapidly due to the environmental changes and due to dust [23]. HV-IGBTs [22] can also be used as a switch instead of sphere gaps. Capacitor banks were enclosed in polyvinyl chloride conduit (PVC) casing and then crammed with magic epoxy to make insulation level better and to evade from the corona discharge particularly at jagged edges of the capacitors legs due to high voltage as shown in Fig. 5.

Wave shaping circuit was designed using Matlab to get the desired shape of the impulse wave. In this model 11KV, pin type insulator (having capacitance of 25pF) [2] was used as a test object. Chopping sphere gap is connected across the test object for protection, which is able to bypass any impulse greater than 95 KV, as shown in Fig. 7. The shunt is connected with test object to observe its status during the test. If the insulator punctures during the test a large voltage drop will appear across the shunt which can be seen on scope. Resistive-Divider and an oscilloscope are provided for measurement purpose [24].

## 3. Analysis

To analyse the system controllability, observability and stability equivalent model shown in Fig. 8 is considered.

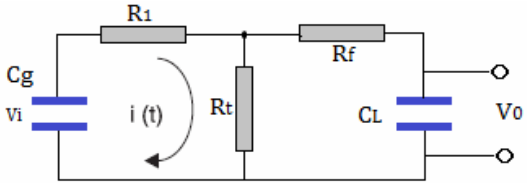


**Fig. 8.** Equivalent Circuit

where,

$C_g$ : IVG equivalent capacitance during discharging state
Vi : Voltage of the impulse generator when it is triggered
$R_1$ : Resistance of sphere gap
$R_f$ : Front resistance
$R_t$ : Tail resistance
Vo : Voltage across the test object
$C_L$ : Load capacitor (Test Object)

### 3.1 Controllability

Using classical control theory controllability of the system can be observed by forming the controllability matrix [25].

$$Mc = [B\ AB] = \begin{bmatrix} \frac{1}{R_1C_1}\left(\frac{1}{R_1C_L}\right)^2 - \frac{1}{R_1^2C_1C_L} & \\ 0 & \frac{1}{R_f^2C_1C_L} \end{bmatrix} \quad (2)$$

Where, $M_C$ is the controllability matrix, A is state matrix of the system and B is the input matrix. It is obvious from the Eq. (2) that the controllability matrix is a diagonal matrix which must be of full rank for any values of $C_L$, $R_f$, $C_1$ and $R_1$. So the system has the unique solution i.e. system is completely controllable.

### 3.2 Observability

Similarly, system observability can be checked by forming the observability matrix [26].

$$Mo = \begin{bmatrix} C \\ A \end{bmatrix} = \begin{bmatrix} 0 & 1 \\ \frac{1}{R_1C_L} & \frac{1}{R_1C_1} \end{bmatrix} \quad (3)$$

Where Mo, is observability matrix, A is state matrix and C is the output matrix of the system. Observability matrix is also diagonal matrix so it must be of full rank irrespective of the elements of the observability matrix. So the system is completely observable.

### 3.3 Stability

Stability of the system can be checked by forming the Lyapunov function [26].

$$A^T M_S + M_S A = -I \quad (4)$$

Where, Ms is stability matrix; A is state matrix while *I* is the identity matrix. By using real values of the system parameters, the system state matrix is:

$$A = \begin{bmatrix} -\frac{2}{3} & \frac{1}{3} \\ \frac{1}{3} & -\frac{2}{3} \end{bmatrix} \quad (5)$$

Solving for the values of $M_S$

$$\begin{bmatrix} -\frac{2}{3} & \frac{1}{3} \\ \frac{1}{3} & -\frac{2}{3} \end{bmatrix}\begin{bmatrix} m_{11} & m_{12} \\ m_{21} & m_{22} \end{bmatrix} + \begin{bmatrix} m_{11} & m_{12} \\ m_{21} & m_{22} \end{bmatrix}\begin{bmatrix} -\frac{2}{3} & \frac{1}{3} \\ \frac{1}{3} & -\frac{2}{3} \end{bmatrix} = \begin{bmatrix} -1 & 0 \\ 0 & -1 \end{bmatrix}$$

Forming equations

$$\frac{1}{3}m_{21} + \frac{2}{3}m_{11} - \frac{2}{3}m_{11} + \frac{1}{3}m_{12} = -1 \quad (6)$$

$$\frac{2}{3}m_{11} + \frac{1}{3}m_{22} - \frac{2}{3}m_{12} + \frac{1}{3}m_{11} = 0 \quad (7)$$

$$\frac{1}{3}m_{11} - \frac{2}{3}m_{21} + \frac{1}{3}m_{22} - \frac{2}{3}m_{21} = 0 \quad (8)$$

$$\frac{1}{3}m_{12} - \frac{2}{3}m_{22} + \frac{1}{3}m_{21} - \frac{2}{3}m_{22} = -1 \quad (9)$$

By solving Eqs. (6)- (8) and (9):

$$M = \begin{bmatrix} \frac{6}{5} & \frac{3}{5} \\ \frac{6}{5} & \frac{6}{5} \end{bmatrix} \quad (10)$$

$$|m_{11}| = \frac{6}{5} > 0, \quad |M| = \frac{18}{25} > 0$$

$A^TM + MA$ is negative definite for a positive definite matrix which satisfies Eq. (4) and also (energy stored approaches to zero) so the system is asymptotically stable.

The Lyapunov function is: L(a) =[$A^T$][M] [a]:

**Table 1.** System parameters

| | |
|---|---|
| Stage capacitors $C_1$ –$C_{120}$ | 220nF |
| Equivalent Capacitance of each stage | 18.33nF |
| Equivalent Capacitance of IVG | 1.833nF |
| Stage resistances | 1000Ω |
| Wavefront resistor | 500Ω |
| Wave tail resistor | 2000Ω |
| Test object capacitance | 25pF |

$$L=\begin{bmatrix}-\frac{2}{3} & \frac{1}{3}\\ \frac{1}{3} & -\frac{2}{3}\end{bmatrix}\begin{bmatrix}\frac{6}{5} & \frac{3}{5}\\ \frac{6}{5} & \frac{6}{5}\end{bmatrix}\begin{bmatrix}a_1\\ a_2\end{bmatrix}=\begin{bmatrix}-\frac{2}{5} & 0\\ 0 & -\frac{3}{5}\end{bmatrix}\begin{bmatrix}a_1\\ a_2\end{bmatrix} \quad (11)$$

$$L(a)=-\frac{1}{5}(2a_1+3a_2)^2 \quad (12)$$

Eq. (12) shows the Lyapunov function which guarantees the stability of the system.

### 3.4 Efficiency

The standard impulse generator equations are given by Kuffel and Zaengl [2].

$$a=\frac{1}{R_t.C_g}+\frac{1}{R_t.C_L}+\frac{1}{R_f.C_g} \quad (13)$$

$$b=\frac{1}{R_t.R_f.C_g.C_L} \quad (14)$$

$$\alpha_1,\alpha_2=\frac{a}{2}\pm\sqrt{\frac{a^2}{4}-b} \quad (15)$$

The output waveform is given by:

$$V_o(t)=\frac{V_i}{R_t.C_L}\frac{1}{(\alpha_2-\alpha_1)}\left[e^{-\alpha_1 t}-e^{-\alpha_2 t}\right] \quad (16)$$

The Marx generator efficiency is defined as:

$$\eta=\frac{V_P}{V_i} \quad (17)$$

Where $V_p$ is the peak output voltage. Practically $C_g>C_L$ and $\alpha_2 \gg \alpha_1$, with these two assumptions, and Eq. (16), the efficiency can be expressed as:

$$\eta=\frac{C_g}{C_g+C_L} \quad (18)$$

In proposed model:

$C_g = 1830$ pF
$C_L = 25$Pf

$$\eta=\frac{1830\,pF}{(1830+25)\,pF}\times 100=98.65\% \quad (19)$$

It is obvious that the efficiency of the proposed Marx impulse circuit is much higher than other generators mentioned earlier.

## 4. Simulation and Experimental Results

Karel Vesiheipl simulated the Marx generator using Pspice [27] but he modeled sphere gaps with simple on/off switches. To use software which can imitate close to the practical effects considering all the factors was a challenge especially to model the sphere gaps. MATLAB/Simulink was selected due to its versatility for simulations. In order to design the proposed model, Marx circuit is modeled in MATLAB/Simulink. Fig. 9 is a simplified equivalent model of the system modeled in Matlab. Sphere gap can be modeled as an ideal switch in MATLAB/Simulink as shown in Fig. 9. This ideal switch can be configured to get the same parameters that a real sphere gap have, like its off time resistance, on time resistance, holding current, capacitance, breakdown voltage, breakdown time etc.

Fig. 10 is an inclusive model of the system. In the real system, a triggering circuit is introduced at first sphere gap to trigger the generator when all the stages are fully charged. Once the first gap is triggered other gaps triggered simultaneously, because voltage adds up and become

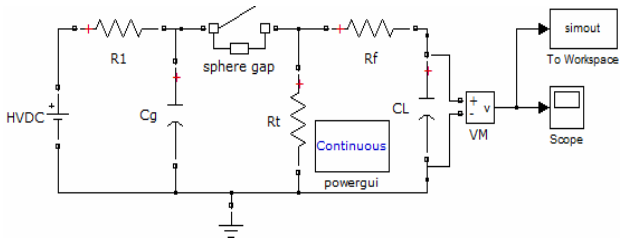


**Fig. 9.** Equivalent Circuit in Matlab/Simulink

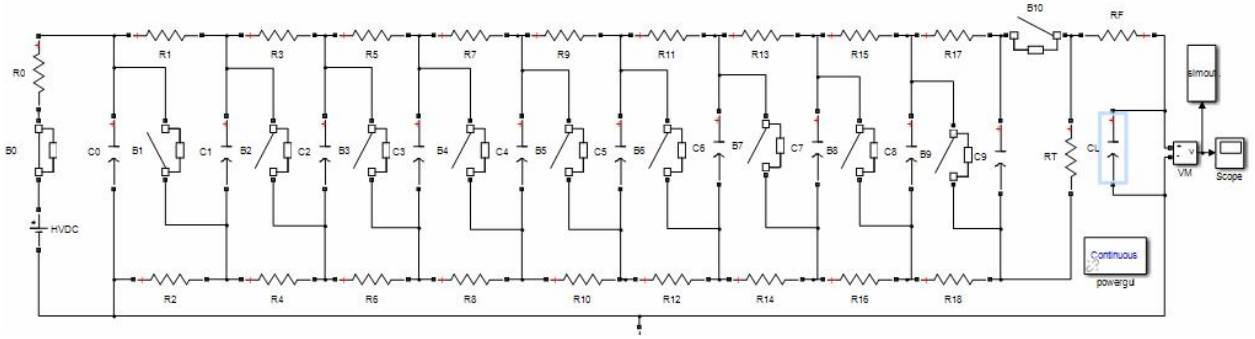


**Fig. 10.** Complete ten stage Model in MATLAB

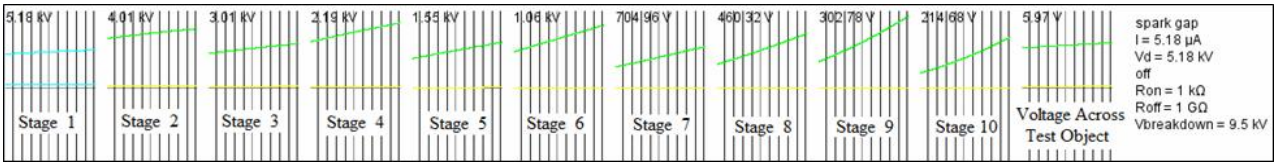


**Fig. 11.** Stage voltages at initial state of charging

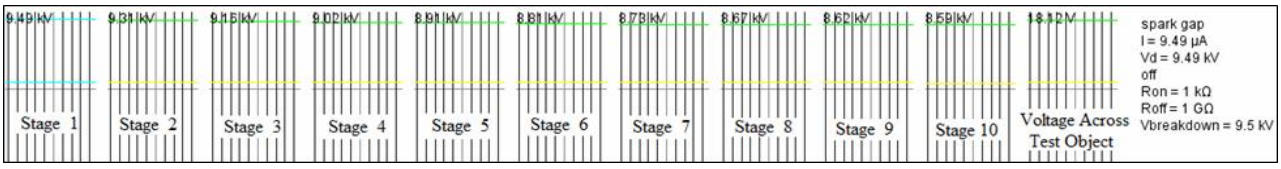


**Fig. 12.** Stage voltages just before the generator is triggered

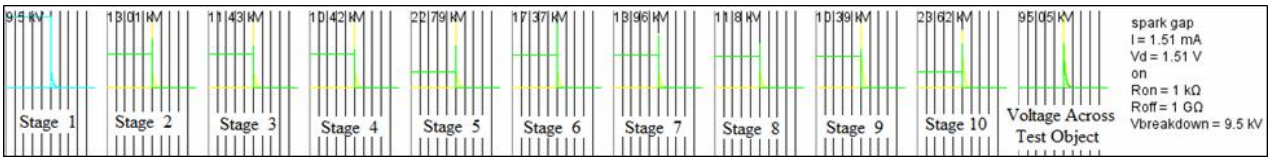


**Fig. 13.** Stage voltages just after the generator is triggered

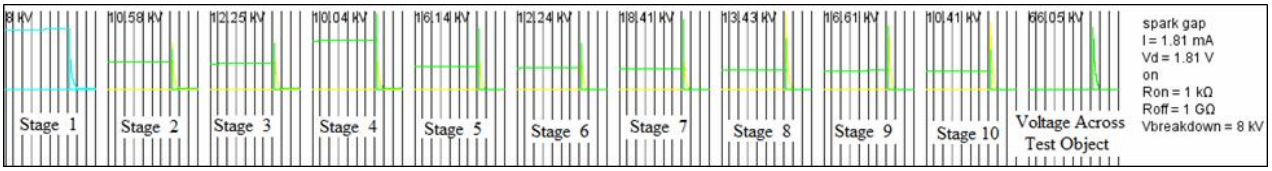


**Fig. 14.** Regulating the output voltage by changing the breakdown voltage of sphere gaps

greater than their breakdown voltage.

Fig. 11 shows the voltages of each stage during the charging stage of the IVG. Fig. 12 depicts voltage levels of all the stages when they are charged up to their rated value. The breakdown voltage of the first gap is set to 9.5 KV that limits the output voltage less or equal to 95 KV.

Fig. 13 shows the state of the voltage levels at the moment when generator is triggered. In Fig.11, 12, 13 and 14 green line shows voltages across sphere gaps while yellow line shows the current through the sphere gaps. Output voltage can be controlled by changing the breakdown voltages of the first sphere gap as shown in Fig. 14.

When all the stages are fully charged up to their rated voltage, a triggering pulse cause breakdown at first stage, breakdown at first stage connects the first two stages in series and results a breakdown on next stage and so on. This process takes place simultaneously and it adds the voltage of all the stages by connecting them in series. So if the breakdown voltage of the first gap set to a lower value it will not allow enough time to the remaining stages to charge up to their rated value, even if the breakdown voltage of the remaining stages are at their rated value.

If the breakdown voltage of the first sphere gap is set to 10KV or greater, all the other stages will be charged up to their rated values that can provide maximum peak impulse voltage. In a small range, output voltage can also be

**Table 2.** Influence of wave shaping resistors

| $R_t$ | $R_f$ | $T_1$(µsec) | $T_2$(µsec) | Output(KV) |
|---|---|---|---|---|
| 250Ω | 1K Ω | 0.93 | 29.56 | 96.73 |
| 500 Ω | 2K Ω | 1.38 | 49.43 | 95.03 |
| 1KΩ | 5K Ω | 7.85 | 57.6 | 94.17 |

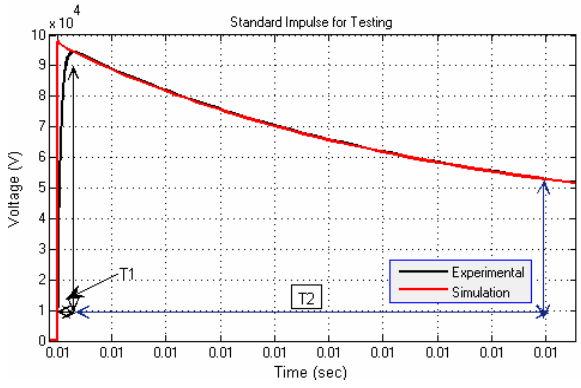


**Fig. 15.** 95 KV standard impulse for testing [$T_1$= front time, $T_2$ = tail time], [$R_1$=1KΩ, $R_f$ =250Ω, $R_t$ = 3KΩ, $C_L$ = 25pF, $C_g$ = 1.83nF]

regulated with a suitable combination of wave front and wave tail resistors as shown in Table 2, but the first method gives wider control of voltage regulation.

Fig. 15 illustrates the wave shape generated in MATLAB at designed values of $R_f$ and $R_t$. Wave front and wave tail time can be controlled by setting the values Rf and Rt.

Fig. 16 shows the variation in wave front time with the variation of wave front resistance by keeping the other parameters constant. Fig. 17 shows the effect of the $R_t$ on wave tail keeping the others parameters constant.

Results show that wave front time can be controlled by changing the $R_f$ and wave tail time can be controlled by Rt, as mentioned in previous literatures. By using suitable values of $R_f$ and Rt any required impulse wave shape can be generated. Variable wave tail and wave front can provide a wider control on the output wave shape. The parasitic capacitance of resistances and the structure is neglected in this work for simplicity.

Proposed experimental model is shown in Fig. 18. This set is suitable for field work due to its light weight, the feasibility of transportation and friendly operation. Table 1 shows the system parameter and values of wave front and wave tail resistors to generate standard lightning impulse wave for testing. Table 2 show the effect of the wave shaping resistor over the performance of the impulse voltage generator. It is clear that with the increase in the values of wave shape resistors, the output voltage wave takes more time to reach the peak magnitude and also decay with a slow rate.

It is clear from Table 3 that the results of the proposed model is well in limits with the simulated results while reducing the system cost and size. System specifications are illustrated in Table 4.

When the peak of the impulse is greater than 95KV it is chopped (bypass) by the chopping sphere gap which protects the test object as shown in Fig. 18. There is a little

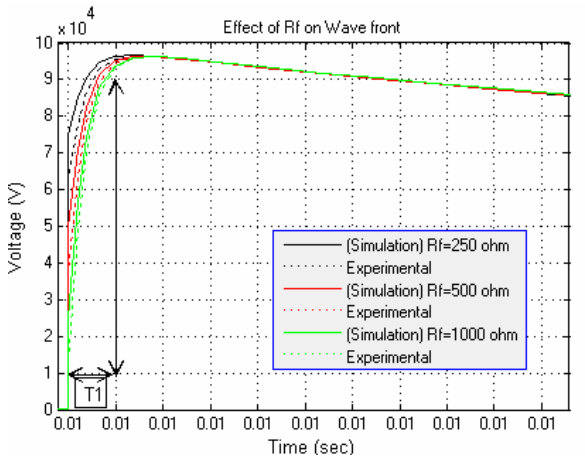


**Fig. 16.** Effect of $R_f$ on wave front

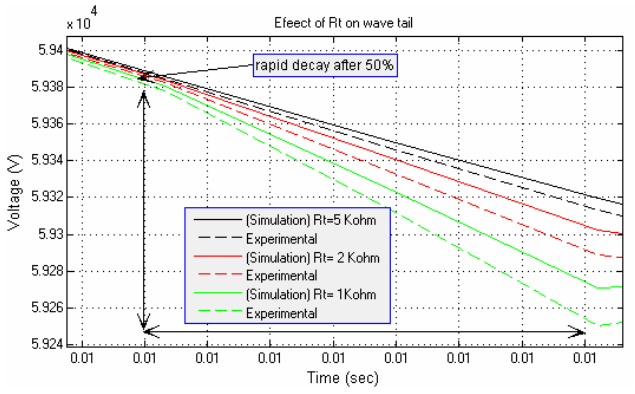


**Fig. 17.** Effect of $R_t$ on wave tail

**Table 3.** Simulation and experimental results comparison

| Gap Setting in KV | | Simulation Output(KV) | Experimental Output(KV) |
|---|---|---|---|
| Gap position | Breakdown voltage (KV) | | |
| 1 | 9.5 | 9.49 | 9.31 |
| 2 | 10 | 9.31 | 9.25 |
| 3 | 10 | 9.15 | 9.18 |
| 4 | 10 | 9.01 | 9.04 |
| 5 | 10 | 8.89 | 8.87 |
| 6 | 10 | 8.79 | 8.60 |
| 7 | 10 | 8.71 | 8.53 |
| 8 | 10 | 8.65 | 8.27 |
| 9 | 10 | 8.60 | 8.02 |
| 10 | 10 | 8.57 | 7.81 |
| Chopping | 95 | 95.05 | 93.81 |

**Table 4.** System specifications and performance

| | | |
|---|---|---|
| Dimensions | Base | 22" x 15" |
| | Top | 20" x 13" |
| | Height | 6' 2" |
| Performance | Input | 230 VAC |
| | Output | 95 KV |
| | Energy | 9.165 Joule |
| | Power consumption | 280 watt |
| | Efficiency (overall) | 82% |
| Weight | 12Kg | |

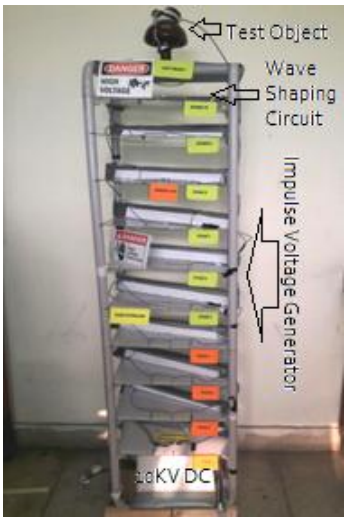


**Fig. 18.** Proposed experimental prototype

delay in the chopped waveform that is due the capacitance of the chopping gap and resistance of the arc.

## 5. Conclusion

In this work, the entire circuit is simulated and modeled based on the circuit parameters which were mathematically calculated. The calculated parameters and their effects on characteristics of the impulse wave is studied and it is found that with proper assumptions and the method followed in the work, the standard impulse wave can be generated. A ten stage impulse generator is designed, simulated, and implemented to verify the effectiveness of the proposed model which gives impulse of 95KV at +10KV DC charging voltage. MATLAB/ (Simulink) simulation clarified the results and these results are compared with the equivalent hardware setup. The proposed model can generate the same results as previous models even the capacitance of the IVG is distributed in every stage of the IVG, which makes it cheaper and more efficient than previous models. The output wave shape of the circuit is very close to the IEC standard wave shape for both lightning and switching impulse. An impulse generator can be developed at very low cost and small in size if this proposed type of method is used. The developed system has the advantages of high efficiency, long lifetime, small in size, high parameter flexibility and low cost. This research effort can be more stretched out by doing enhancements in the circuit with the help of altered Marx circuits (using distributed charging resistances), which won't just make the outline more compact and versatile additionally wave shapes will also be controlled. If the stage resistances are more distributed all throughout the circuit it will provide more accurate control on wave shapes. It can also overcome the parasitic capacitance effect which hinders the wave shapes.

## Acknowledgements

This work is supported by the National Natural Science Foundation of China (NSFC) (Grant No. 51777166).

## References

[1] J. Ma, Q. Zhang, H. You, Z. Wu, T. Wen, C. Guo, et al., "Study on insulation characteristics of GIS under combined voltage of DC and lightning impulse," *IEEE Transactions on Dielectrics and Electrical Insulation*, vol. 24, pp. 893-900, 2017.

[2] J. Kuffel and P. Kuffel, High voltage engineering fundamentals: Newnes, 2000.

[3] *S. Boggs and J. Y. Zhou, "Dielectric property* measurement of nonlinear grading materials," *in Electrical Insulation and Dielectric Phenomena, 2000 Annual Report Conference on*, 2000, pp. 764-767.

[4] G. Lopes, G. Faria, E. Neto, and M. Martinez, "Lightning withstand of medium voltage cut-out fuses stressed by nonstandard impulse shapes experimental results," *in IEEE Electrical Insulation Conference* (*EIC*), 2016, 2016, pp. 210-214.

[5] J. Li, L. Zhang, D. Hu, X. Yao, J. Xiong, and S. Wang, "Breakdown characteristics of SF6 in quasi-uniform field under oscillating lightning impulse voltages," *IEEE Transactions on Dielectrics and Electrical Insulation*, vol. 24, pp. 915-922, 2017.

[6] P. Rozga and M. Stanek, "Comparative analysis of lightning breakdown voltage of natural ester liquids of different viscosities supported by light emission measurement," *IEEE Transactions on Dielectrics and Electrical Insulation*, vol. 24, pp. 991-999, 2017.

[7] B. Qi, X. Zhao, S. Zhang, M. Huang, and C. Li, "Measurement of the electric field strength in transformer oil under impulse voltage," *IEEE Transactions on Dielectrics and Electrical Insulation*, vol. 24, pp. 1256-1262, 2017.

[8] Y. Liu, L. Lee, Y. Bing, Y. Ge, W. Hu, and F. Lin, "Resonant charging performance of spiral tesla transformer applied in compact high-voltage repetitive nanosecond pulse generator," *IEEE Transactions on Plasma Science*, vol. 41, pp. 3651-3658, 2013.

[9] L. Collier, J. Dickens, J. Mankowski, and A. Neuber, "Performance Analysis of an All Solid-State Linear Transformer Driver," *IEEE Transactions on Plasma Science*, vol. 45, pp. 1755-1761, 2017.

[10] L. Redondo, H. Canacsinh, and J. F. Silva, "Generalized solid-state marx modulator topology," *IEEE Transactions on Dielectrics and Electrical Insulation*, vol. 16, pp. 1037-1042, 2009.

[11] H. Li, Y. Wang, W. Chen, W. Luo, Z. Yan, and L. Wang, "Inductive pulsed power supply consisting of superconducting pulsed power transformers with Marx generator methodology," *IEEE Transactions on Applied Superconductivity*, vol. 22, pp. 5501105-5501105, 2012.

[12] Y. Xuelin, D. Zhenjie, H. Qingsong, Y. Jianguo, Z. Bo, and H. Long, "High-repetition and-stability all-solid state pulsers based on avalanche transistor Marx circuit," *in Microwave and Millimeter Wave Technology* (*ICMMT*), 2010 International Conference on, 2010, pp. 454-455.

[13] J. Casey, F. Arntz, M. Kempkes, and M. Gaudreau, "Conference Record of the 2006 Twenty-Seventh International Power Modulator Symposium."

[14] T. Prabaharan, A. Shyam, R. Shukla, P. Banerjee, S. Sharma, P. Deb, et al., "Development of 2.4 ns rise time, 300 kV,~500 MW compact co-axial Marx generator," 2011.

[15] S. Roy and A. Debnath, "Procedural Perfection in Impulse Shape Generation for Indoor Type Impulse

Test of Power Transformers," *Global Journal of Research In Engineering*, vol. 10, 2010.
[16] C. Wang, X. Zheng, J. Zou, J.-z. Wang, T.-j. Zhang, and X.-d. Jiang, "Design and construction of a compact portable pulsed power generator," *Nuclear Instruments and Methods in Physics Research Section B: Beam Interactions with Materials and Atoms*, vol. 269, pp. 2941-2945, 2011.
[17] A. Toudeshki, N. Mariun, H. Hizam, and N. I. A. Wahab, "The energy and cost calculation for a Marx pulse generator based on input DC voltage, capacitor values and number of stages," *in Power and Energy* (*PECon*), *2012 IEEE International Conference on,* 2012, pp. 745-749.
[18] J. Y. Zhou and S. A. Boggs, "Low energy single stage high voltage impulse generator," *IEEE transactions on dielectrics and electrical insulation*, vol. 11, pp. 597-603, 2004.
[19] J. M. Beck, "Using rectifiers in voltage multiplier circuits," *General Semiconductor*, vol. 14, 2001.
[20] D. F. Spencer, R. Aryaeinejad, and E. Reber, "Using the Cockroft-Walton voltage multiplier design in handheld devices," *in Nuclear Science Symposium Conference Record*, *2001 IEEE*, 2001, pp. 746-749.
[21] G. Swift, "Charging time of a high-voltage impulse generator," *Electronics Letters*, vol. 5, pp. 534-534, 1969.
[22] H. Canacsinh, L. Redondo, F. F. Silva, and E. Schamiloglu, "Modeling of a solid-state Marx generator with parasitic capacitances for optimization studies," *in Pulsed Power Conference* (*PPC*), 2011 IEEE, 2011, pp. 1422-1427.
[23] T. Rokunohe, T. Kato, H. Kojima, N. Hayakawa, and H. Okubo, "Calculation model for predicting partial-discharge inception voltage in a non-uniform air gap while considering the effect of humidity," *IEEE Transactions on Dielectrics and Electrical Insulation*, vol. 24, pp. 1123-1130, 2017.
[24] Y. Liu, F. Lin, G. Hu, and M. Zhang, "Design and performance of a resistive-divider system for measuring fast HV impulse," *IEEE Transactions on Instrumentation and Measurement*, vol. 60, pp. 996-1002, 2011.
[25] D. Cobb, "Controllability, observability, and duality in singular systems," *IEEE Transactions on Automatic Control*, vol. 29, pp. 1076-1082, 1984.
[26] J. Daafouz, P. Riedinger, and C. Iung, "Stability analysis and control synthesis for switched systems: a switched Lyapunov function approach," *IEEE transactions on automatic control*, vol. 47, pp. 1883-1887, 2002.
[27] K. Veisheipl, "Simulation of the high voltage impulse generator," *in Electric Power Engineering* (*EPE*), 2016 17th International Scientific Conference on, 2016, pp. 1-5.

**Zahid Javid** (Student Member IEEE) received the B.Sc. degree in electrical engineering from university of Engineering & Technology Lahore, Pakistan, in 2015. Currently, he is pursuing his M.S. Electrical in Power system and automation in Shandong University, Jinan, China

**Ke-Jun Li** (M'07-SM'15) received the B.S. and M.S. degrees from Shandong University of Technology, Jinan, China, and the Ph.D. degree from Shandong University, Jinan, China, in 1994, 1999, and 2005, respectively, all in Electrical Engineering. From 2007 to 2008, He was a post-doctoral researcher in the department of electrical engineering at the University of Texas at Arlington, TX, USA. He is currently a Professor with the School of Electrical Engineering and the Deputy Director of Institute of Renewable Energy and Smart Grid, Shandong University, China.
Prof. Li has been involved in research on renewable energy integration, microgrid operation and control, modeling and control for HVDC and FACTS devices, on-line equipment protection, monitoring, and control system.

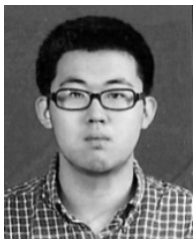

**Kaiqi Sun** (Student Member IEEE) received the B.Sc. degree in electrical engineering from Shandong University, Jinan, China, in 2015. He is currently working toward the Ph.D. degree at Shandong University. His research interests include the control strategy of HVDC system, the application of VSC-MTDC systems for renewable energy integration and urban power grid.

**Arooj Unbreen** received the B.Sc. degree in electrical engineering from university of Engineering & Technology Lahore, Pakistan, in 2015. Currently, she is pursuing her M.S. degree in Electrical Engineering.